



Synthesis of graphene-supported LiFePO_4/C materials via solid-state method using $\text{LiFePO}_4(\text{OH})$ as precursors

Yuanchao Li^{1,2} · Baoyan Xing¹ · Pengchao Liang¹ · Huishuang Zhang² · Kaiyang Zhou¹ · Jingjing Ma¹ · Shumin Fan¹ · Shuting Yang²

Received: 17 October 2021 / Revised: 8 July 2022 / Accepted: 6 August 2022 / Published online: 11 August 2022
© The Author(s), under exclusive licence to Springer-Verlag GmbH Germany, part of Springer Nature 2022

Abstract

The solid-state method is a mainly adopted large-scale preparation of LiFePO_4 cathode materials for Li-ion batteries but suffers from a challenge of irregular morphology and particle agglomeration. Herein, a graphene-supported $\text{LiFePO}_4/\text{C}@G$ composite with uniform morphology and electronic conducting network was synthesized via a freeze-drying assisted solid-state method without ball milling using the integrated $\text{LiFePO}_4(\text{OH})$ as precursor. The integrated $\text{LiFePO}_4(\text{OH})$ as precursor may avoid segregation of element caused by inhomogeneous mixing of raw materials in the process of solid-state preparation. The as-prepared graphene-coated $\text{LiFePO}_4/\text{C}@G$ shows excellent electrochemical properties with a specific capacity of 156, 154, 150, 145, 139, 132 mA h g^{-1} at 0.1, 0.2, 0.5, 1, 2, 5 C and a capacity retention of around 97.0% for 200 cycles at 2 C. This can be attributed to uniform element distribution and continuous electronic conducting network. The freeze-drying assisted solid-phase method using $\text{LiFePO}_4(\text{OH})$ precursor and graphene is a promising route for production of LiFePO_4/C materials with excellent performances.

Keywords LiFePO_4 · $\text{LiFePO}_4(\text{OH})$ · Graphene · Cathode materials · Lithium-ion batteries

Introduction

Lithium ferrous phosphate (LiFePO_4) cathode material is considered to be one of the most promising cathode materials for lithium-ion power batteries due to the abundant raw materials, high safety, environmental friendliness. However, low electron conductivity and ion diffusion limit the electrochemical properties of LiFePO_4 materials, hindering the commercialization process [1]. Effective strategy to improve the conductivity of LiFePO_4 is proven to be carbon coating along with preferential nanocrystallization [2–6] and ion

doping [7–9], which can make the electrochemical performances of LiFePO_4 materials reach a level of commercial application. At present, the cost and stability of its preparation process are still a bottleneck of limiting its large-scale application compared to conventional lead-acid and nickel-hydrogen batteries [10, 11]. Therefore, it is essential for a wide industrial application to develop an inexpensive and facile solid-state method to produce a uniform LiFePO_4 material without particle agglomeration.

Although many researchers have reported many procedures of synthesizing LiFePO_4 , such as spray pyrolysis [12], combination of spray pyrolysis and ball-milling [13], spray drying [14], sol-gel [15], coprecipitation [16] and conventional solid-state reaction method [17], the synthesis method of LiFePO_4 materials can be generally divided into solid state reaction and solution method. Solution method usually is accompanied with complex preparation process, leading to the high cost of preparation [10]. Accordingly, the large-scale preparation mainly adopts solid state method, although the solid state method encountered some application issues such as particle agglomeration with irregular morphology [5, 18]. In a conventional solid-state process of preparation, an iron source, phosphorus source

✉ Yuanchao Li
liyuanchoozu@126.com

✉ Shuting Yang
shutingyang@foxmail.com

¹ School of Chemistry and Chemical Engineering, Henan Institute of Science and Technology, Xinxiang 453003, People's Republic of China

² School of Chemistry and Chemical Engineering, Collaborative Innovation Center of Henan Province Motive Power and Key Materials, Henan Normal University, Xinxiang 453007, People's Republic of China

and Li source are used as starting materials for synthesizing LiFePO_4 materials. Before it is decomposed at a temperature ranging from 600 to 700 °C for 8–15 h, a precursor is usually obtained via mixing the starting materials through ball milling. The ball milling can help both homogeneity and reduction of the particle size. However, the ball milling often brings about irregular morphology and particle agglomeration, resulting in unstable electrochemical performances [19]. In addition, ball milling also increases the cost of material preparation. To reduce irregular morphology and the particle agglomeration of LiFePO_4 materials in conventional solid-state method, the introduction of integrated materials containing the Li, Fe, P elements as raw materials, such as $\text{LiFePO}_4(\text{OH})$, is very necessary. The $\text{LiFePO}_4(\text{OH})$ was first reported by Whittingham to be formed through the reaction of $\text{FePO}_4 \cdot \text{H}_2\text{O}$ and CH_3COOLi in hydrothermal process [20]. Subsequently it was found that nano-sized LiFePO_4 reacts with H_2O to form $\text{LiFePO}_4(\text{OH})$ in a wet environment [21, 22], and the $\text{LiFePO}_4(\text{OH})$ could still be reverse-reacted to LiFePO_4 after high-temperature heat treatment [22]. Next, $\text{LiFePO}_4(\text{OH})$ or $\text{LiFe}(\text{PO}_4)_x(\text{OH})_{1-x}$ was synthesized by solvothermal method [23–25]. After mixing it with carbon, the $\text{LiFePO}_4(\text{OH})$ was electrochemically active, with a specific capacity of 130 mA h g^{-1} at 0.1C. Another research on $\text{LiFePO}_4(\text{OH})$ has suggested that it can also be obtained by $\text{FePO}_4 \cdot \text{H}_2\text{O}$ through H^+/Li^+ exchange [26]. In addition, the effective strategy to relieve the sluggish kinetics of LiFePO_4 is to integrate LiFePO_4 and graphitized carbonaceous materials with large contact area such as graphene and carbon nanotubes [27–29], which is widely applied for synthesizing high-rate hybrid electrodes with the least carbon content. For instance, the graphene-modified LiFePO_4 materials were fabricated and promoted the improvement of its overall electrochemical performance [28, 30]. To the best of our knowledge, no research on using the integrated $\text{LiFePO}_4(\text{OH})$ as a precursor for synthesizing LiFePO_4 material has been reported. Based on the above considerations, we applied the integrated $\text{LiFePO}_4(\text{OH})$ compound containing Li, Fe, P elements as precursor, so that a morphology-inherited LiFePO_4 material with uniform element distribution can be obtained without ball milling.

Herein, a graphene-supported $\text{LiFePO}_4/\text{C}@G$ composite with uniform element distribution is successfully synthesized using the integrated $\text{LiFePO}_4(\text{OH})$ and the sucrose in graphene oxide (GO) suspension as raw materials. The as-prepared $\text{LiFePO}_4/\text{C}@G$ exhibits excellent electrochemical performances due to uniform particle and electronic conducting network formed with graphene and surface coating carbon layer. This provides a reference for large-scale preparation route of LiFePO_4/C materials.

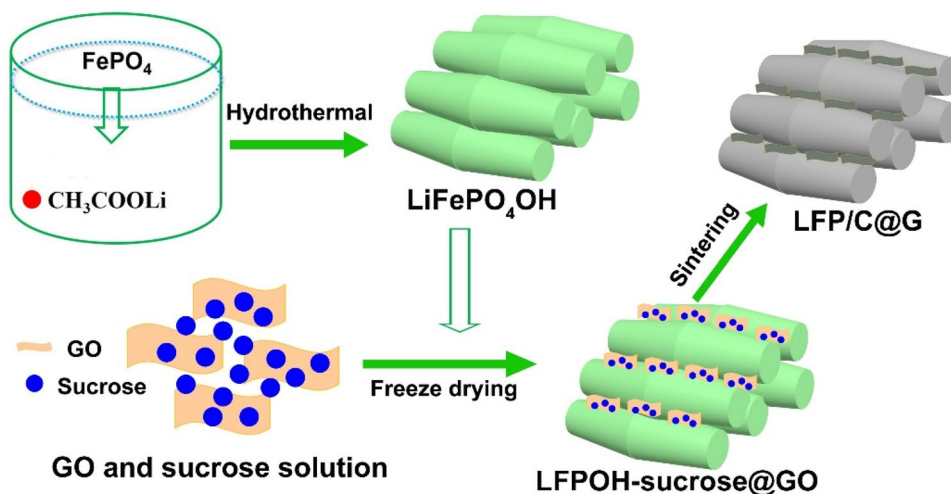
Experimental

The LiFePO_4OH precursor was prepared by hydrothermal method using $\text{FePO}_4 \cdot 2\text{H}_2\text{O}$ and CH_3COOLi as raw materials. Specifically, 0.006 mol of CH_3COOLi was dissolved in 120 ml of deionized water. Then, stoichiometric $\text{FePO}_4 \cdot 2\text{H}_2\text{O}$ (0.006 mol) was added into the above solution under continuous stirring for 30 min. Then, the total solution was transferred into a 200 ml of stainless-steel autoclave, sealed and heated at 180 °C for 72 h. The resultant product was washed with deionized water for several times and was dried in a vacuum at 80 °C, before the LiFePO_4OH precursor was obtained. After it was mixed with 14 wt% of sucrose in 3 wt% graphene oxide (GO) suspension, the obtained mixture was freeze-dried and calcined at 700 °C for 10 h under N_2 atmosphere. Finally, the $\text{LiFePO}_4/\text{C}@G$ composite was obtained. The LiFePO_4/C was synthesized via the same procedure except without adding GO for comparison.

The crystalline phases of the samples were identified by a PANalytical X'PertPro X-ray diffractometer (Cu K α radiation, 40 kV). The particle morphologies of the samples were examined by field emission scanning electron microscopy (FE-SEM, Hitachi S-4800). X-ray photoelectron spectroscopy (XPS) data were collected by a PHI Quantera SXM spectrometer using the C 1s peak with 284.8 eV, and the corresponding fitted spectra were carried out by using XPSPEAK 4.1 software. Thermogravimetric analysis (TGA) was measured using STA 449F3 analyzer (NETZSCH Co.) under air atmosphere to obtain carbon content of composites at a heating rate of $10 \text{ }^\circ\text{C min}^{-1}$.

The electrochemical tests were investigated by assembling CR2016 coin-type cells. The cathode electrode was fabricated by coating aluminum foil with the slurry composed of 80 wt% of active material LiFePO_4/C , 10 wt% of polyvinylidene binder and 10 wt% of Super-P in *N*-methyl-2-pyrrolidone. After drying at 120 °C for 12 h in a vacuum, the electrode was punched into disc with the diameter of 14 mm as the cathode. Lithium foil served as the counter electrode, and Celgard 2400 membrane was used as the separator. The electrolyte is consisted of a solution of 1 M LiPF_6 in EC and DMC (volume ratio of 1:1). The buttoned batteries (CR2016) were assembled in a glove box filled with argon. After the assembled batteries were laid aside for 3 h, the electrical performance of batteries were tested on the batteries tester (Land CT 2001A, Land Co. China) under a voltage range of 2.0–4.5 V. Cyclic voltammetry and AC impedance spectroscopy measurements were performed at electrochemical workstation (CHI604E, Chenhua, China). The amplitude and frequency range of AC impedance are 5 mV and 0.1–100 kHz, respectively.

Scheme 1 Schematic illustration for synthesis of the LFP/C@G sample



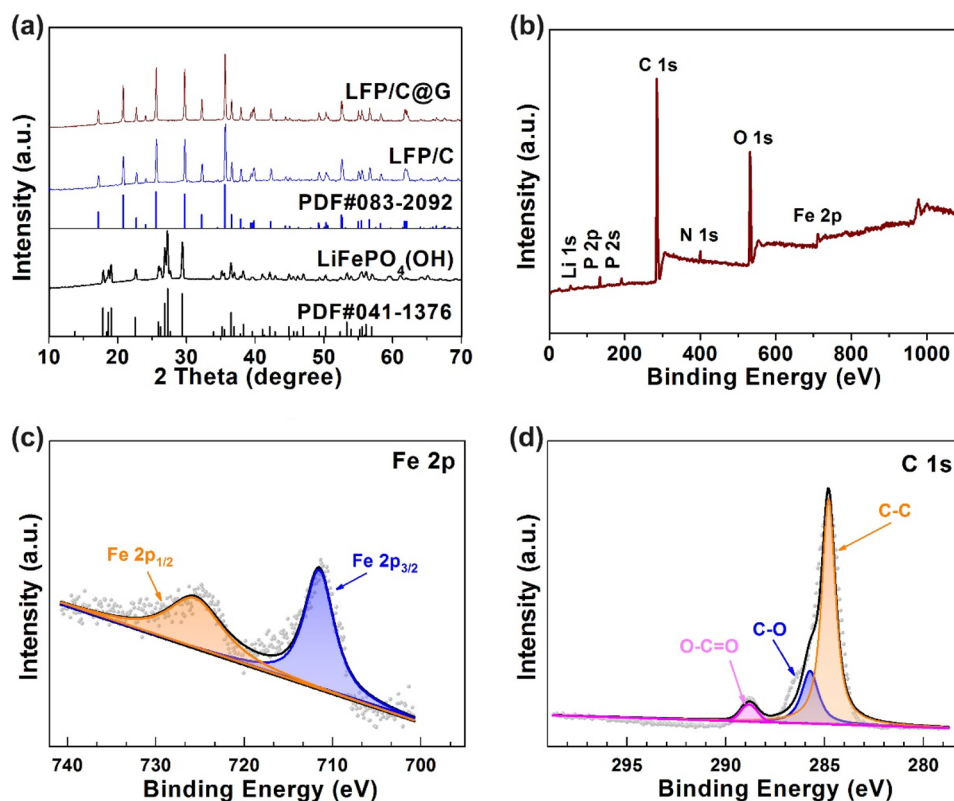
Results and discussion

The preparation process is shown in Scheme 1. To solve component segregation of the raw materials and improve the consistency of the LiFePO_4 materials in mixing in solid-state preparation method of LiFePO_4 materials, a strategy was proposed that the reaction phases were reduced in the mixing of raw materials through using $\text{LiFePO}_4(\text{OH})$ containing Li, Fe and P as precursor. $\text{LiFePO}_4(\text{OH})$ precursor was prepared by hydrothermal method using FePO_4 and CH_3COOLi as raw

materials, followed by thermal conversion of $\text{LiFePO}_4(\text{OH})$ in the presence of sucrose in graphene-supported LiFePO_4/C composite.

Figure 1 presents XRD patterns of the $\text{LiFePO}_4(\text{OH})$ precursor, LFP/C and LFP/C@G samples. As shown in Fig. 1, the diffraction peaks of the as-prepared $\text{LiFePO}_4(\text{OH})$ samples match well with the standard diffraction peaks of $\text{LiFePO}_4(\text{OH})$ (JCPDS No. 041–1376), indicating the high purity of the prepared $\text{LiFePO}_4(\text{OH})$ sample. $2\theta = 17.82^\circ$, 18.59° , 19.02° , 22.53° , 25.90° , 26.80° , 27.23° , 29.38° and

Fig. 1 XRD patterns for the as-prepared samples (a) as well as XPS survey (b) and high-resolution elemental of Fe 2p (c) and C 1s (d) for the LFP/C@G



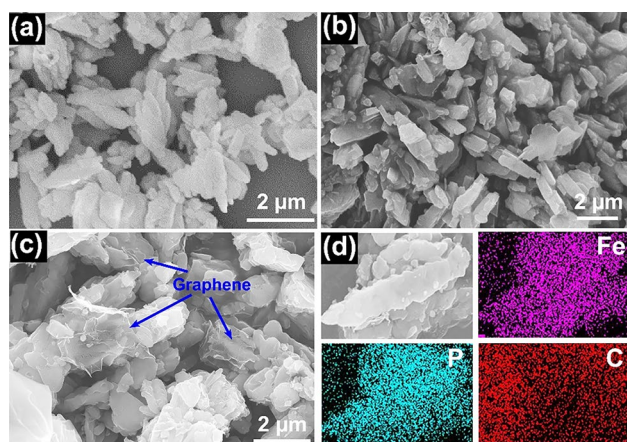


Fig. 2 SEM image of $\text{LiFePO}_4(\text{OH})$ raw material (a), LFP/C (b) and LFP/C@G (c) as well as EDS images (d) of the LFP/C@G

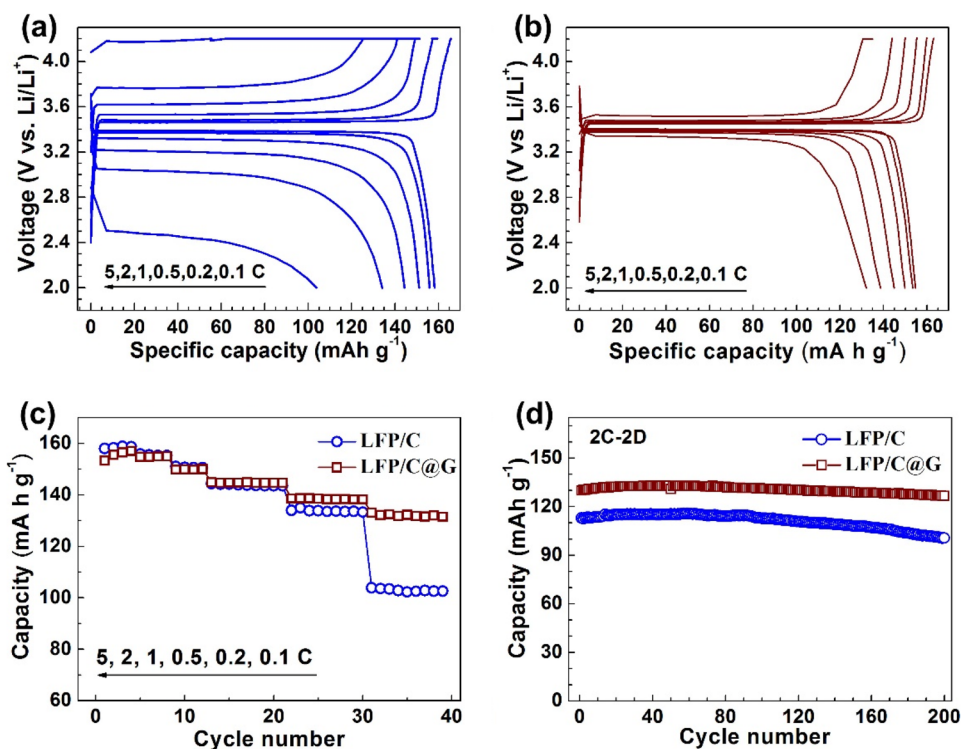
36.47° positions correspond to the characteristic diffraction peaks of (100), (011), (001), (-101), (111), (021), (-120), (101) and (-201) crystal planes, respectively. In addition, the diffraction peaks of the obtained LFP/C and LFP/C@G samples from $\text{LiFePO}_4(\text{OH})$ also are well indexed to olivine structured LiFePO_4 with space group Pnma (JCPDS 83–2092). This indicates that LiFePO_4/C composites with high purity can be synthesized using $\text{LiFePO}_4(\text{OH})$ with Li, Fe and P elements as raw material. XPS spectrum was obtained to verify the elemental compositions and chemical states, shown in Fig. 1b–d. The XPS survey spectrums of the $\text{LiFePO}_4/\text{C}@G$

sample show the typical peaks for Fe 2p, C 1s, P 1s and O 1s, respectively. In the high-resolution spectrum of the Fe 2p, two peaks located at about 711 and 724 eV, matching to $\text{Fe } 2p_{3/2}$ and $\text{Fe } 2p_{1/2}$, which may be ascribed to Fe (II) state [31]. In Fig. 1d, the peak for C 1s at 284.7, 286.1 and 288.7 eV can be regarded as C–C band, C–O band and O–C=O band, which evidences the presence of the modified graphene [30].

Figure 2 shows SEM images of the $\text{LiFePO}_4(\text{OH})$ precursor and carbon-coated LiFePO_4/C material. As seen from Fig. 2a, $\text{LiFePO}_4(\text{OH})$ precursor possesses uniform spindle-shaped morphology with 2 μm in length and 300 nm in width. There is a smooth surface with no other impurity phase on the material particles. In Fig. 2b, SEM images of the carbon-coated LFP/C sample shows little different morphology compared with the $\text{LiFePO}_4(\text{OH})$ precursor. This indicates that the morphology of LFP/C materials can be regulated by $\text{LiFePO}_4(\text{OH})$ precursor. In order to further improve the rate performance of LFP/C, GO was added to the LFP/C sample, and its SEM was shown in Fig. 2c. In Fig. 2c, graphene can be observed in the LFP/C@G sample, indicating that the graphene is successfully coated on the surface of LFP/C particles. The EDS results of LFP/C@G in Fig. 2d show that C, P and Fe are uniformly distributed in the LFP/C@G sample. Therefore, the $\text{LiFePO}_4(\text{OH})$ precursor can be used as raw materials for synthesizing uniform LiFePO_4/C materials without the ball milling, which is beneficial for engineering application [32, 33].

Figure 3 shows rate capability and cycling performances of the LFP/C and LFP/C@G samples synthesized from $\text{LiFePO}_4(\text{OH})$ precursor. In Fig. 3a, the LFP/C sample shows

Fig. 3 Charge/discharge curves for LFP/C (a) and LFP/C@G (b) as well as their rate capability (c) and cycling performance (d)



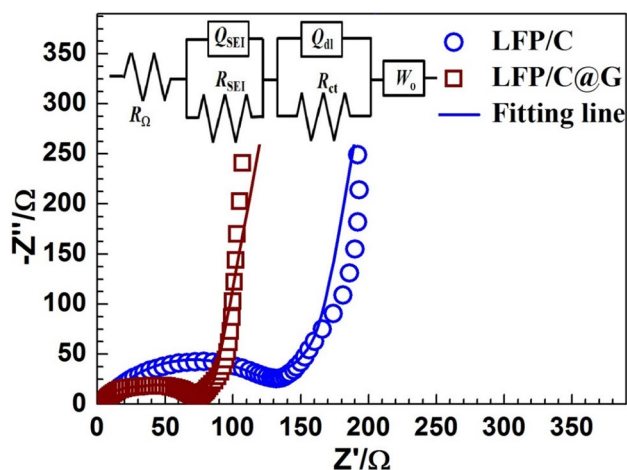


Fig. 4 EIS plots of LFP/C and LFP/C@G samples

an initial specific capacity of 158 mA h g^{-1} at rate of 0.1 C (close to theoretical capacity of 170 mA h g^{-1}), indicating a high purity of the as-prepared LFP/C sample, while the LFP/C sample just maintains a specific capacity of 135 and 106 mA h g^{-1} at a high rate of 2 and 5 C, respectively and shows a great polarization with merely a voltage platform of 2.5 V at 5 C, indicating that the rate performance of the LFP/C sample needs to be further improved. It is worthy of mentioning that the carbon content of the LFP/C and LFP/C@G samples is calculated to be 1.49 and 4.37 wt% from the thermogravimetric (TGA) curves (Fig. S1), respectively [34]. Therefore, the inferior rate performance of LFP/C sample may be mainly due to the low electronic conductivity resulting from less carbon content of only 1.49 wt%. To further improve the rate performance of the LFP/C sample, GO was added to the LFP/C sample for synthesizing the graphene-supported LiFePO_4/C composite (LFP/C@G). In Fig. 3b, the LFP/C@G delivers a specific capacity of 156, 154, 150, 145, 139, 132 mA h g^{-1} at 0.1, 0.2, 0.5, 1, 2 and 5 C with a higher voltage platform of 3.3 V at 5 C, showing excellent rate performance (Fig. 3c). As shown in Fig. 3d, the specific capacity of the LFP/C@G sample drops from 131 to 127 mA h g^{-1} in the 200 cycles at 2 C, showing a longer capacity retention of 97.0% compared with the LFP/C (capacity retention of 89.2%), indicating better cycling stability for LFP/C@G. The above electrochemical results demonstrate that a LiFePO_4 material with excellent electrochemical performances can be obtained using $\text{LiFePO}_4(\text{OH})$ as precursor combined with graphene modification.

Electrochemical impedance spectroscopy (EIS) of the as-prepared samples was performed in the fully discharged (lithiation) state, as shown in Fig. 4. The EIS profiles consist of a partially overlapped semicircle in the high-frequency region followed by a sloping line in the low-frequency region. The semicircle in the high- and middle-frequency regions is

due to the charge-transfer resistance (R_{ct}). The sloping line in the lower frequency represents the Warburg impedance (W_s) associated with lithium-ion diffusion in the bulk of the electrode [35, 36]. By fitting data, the charge-transfer resistance of LFP/C and LFP/C@G samples was approximately 68 and 130Ω , respectively, indicating better kinetic behavior of the LFP/C@G sample. The EIS result validates that the superior rate performance of LFP/C@G sample results from the improved electrochemical reaction kinetics.

Conclusion

In summary, we prepared a graphene-supported LiFePO_4/C @G composite with uniform morphology and electronic conducting network via a freeze-drying assisted solid-phase method using the integrated $\text{LiFePO}_4(\text{OH})$ as precursor. The as-prepared LFP/C samples show a similar spindle-shaped morphology as the $\text{LiFePO}_4(\text{OH})$ precursor, indicating a feasibility for regulation of the LiFePO_4/C morphology by $\text{LiFePO}_4(\text{OH})$. Moreover, the graphene-supported LiFePO_4/C @G shows better electrochemical properties with a specific capacity of 156, 154, 150, 145, 139, 132 mA h g^{-1} at 0.1, 0.2, 0.5, 1, 2, 5 C, which benefits from the synergetic effect of uniform $\text{LiFePO}_4(\text{OH})$ as precursor and continuous graphene electronic conducting network. The freeze-drying assisted solid-phase method using $\text{LiFePO}_4(\text{OH})$ as precursor without ball milling provides a new insight for solving the problem of particle agglomeration caused by ball milling in solid-state method. The strategy would apply to olivine materials with other transition metals (Mn, Co or Ni).

Supplementary Information The online version contains supplementary material available at <https://doi.org/10.1007/s10008-022-05266-z>.

Funding We are grateful for financial supports from the Programs for Science and Technology Development of Henan Province (No. 192102210016 and 222102240094), the Research Foundation for Key Scientific Research Project of Colleges and Universities of Henan Province (No. 21B480003) and Henan Postdoctoral Science Foundation (No. 001802032).

References

1. Padhi AK, Nanjundaswamy KS, Goodenough JB (1997) Phospho-olivines as positive-electrode materials for rechargeable lithium batteries. *J Electrochem Soc* 144(4):1188–1194
2. Shin HC, Cho WI, Jang H (2006) Electrochemical properties of the carbon-coated LiFePO_4 as a cathode material for lithium-ion secondary batteries. *J Power Sources* 159(2):1383–1388
3. Liu YY, Cao CB, Li J (2010) Enhanced electrochemical performance of carbon nanospheres- LiFePO_4 composite by PEG based sol-gel synthesis. *Electrochim Acta* 55(12):3921–3926
4. Oh SW, Myung ST, Oh SM, Oh KH, Amine K, Scrosati B, Sun YK (2010) Double carbon coating of LiFePO_4 as high rate electrode for rechargeable lithium batteries. *Adv Mater* 22(43):4842–4845

- Yang K, Deng Z, Suo J (2012) Effects of carbon sources and carbon contents on the electrochemical properties of LiFePO_4/C cathode material. *J Solid State Electrochem* 16(8):2805–2813
- Wang L, He X, Sun W, Wang J, Li Y, Fan S (2012) Crystal orientation tuning of LiFePO_4 nanoplates for high rate lithium battery cathode materials. *Nano Lett* 12(11):5632–5636
- Chung S-Y, Bloking JT, Chiang Y-M (2002) Electronically conductive phospho-olivines as lithium storage electrodes. *Nat Mater* 1(2):123–128
- Gao Y, Xiong K, Zhang H, Zhu B (2021) Effect of Ru doping on the properties of LiFePO_4/C cathode materials for lithium-ion batteries. *ACS Omega* 6(22):14122–14129
- Vasquez FA, Calderon JA (2019) Vanadium doping of LiMnPO_4 cathode material: correlation between changes in the material lattice and the enhancement of the electrochemical performance. *Electrochim Acta* 325:134930–134939
- Yuan LX, Wang ZH, Zhang WX, Hu XL, Chen JT, Huang YH, Goodenough JB (2011) Development and challenges of LiFePO_4 cathode material for lithium-ion batteries. *Energy Environ Sci* 4(2):269–284
- Goodenough JB, Park KS (2013) The Li-ion rechargeable battery: a perspective. *J Am Chem Soc* 135(4):1167–1176
- Kashi R, Khosravi M, Mollazadeh M (2018) Effect of carbon precursor on electrochemical performance of LiFePO_4/C nano composite synthesized by ultrasonic spray pyrolysis as cathode active material for Li ion battery. *Mater Chem Phys* 203:319–332
- Muruganatham R, Sivakumar M, Subadevi R (2015) Enhanced rate performance of multiwalled carbon nanotube encrusted olivine type composite cathode material using polyol technique. *J Power Sources* 300:496–506
- Gao F, Tang Z, Xue J (2007) Preparation and characterization of nano-particle LiFePO_4 and LiFePO_4/C by spray-drying and post-annealing method. *Electrochim Acta* 53(4):1939–1944
- Alsamet MAMM, Burgaz E (2021) Synthesis and characterization of nano-sized LiFePO_4 by using consecutive combination of sol-gel and hydrothermal methods. *Electrochim Acta* 367:137530
- Wang S, Yang H, Feng L, Sun S, Guo J, Yang Y, Wei H (2013) A simple and inexpensive synthesis route for LiFePO_4/C nanoparticles by co-precipitation. *J Power Sources* 233:43–46
- Xi Y, Lu Y (2020) Toward uniform in situ carbon coating on nano- LiFePO_4 via a solid-state reaction. *Ind Eng Chem Res* 59(30):13549–13555
- Ati M, Sathiyam M, Boulineau S, Reynaud M, Abakumov A, Rousse G, Melot B, Van Tendeloo G, Tarascon JM (2012) Understanding and promoting the rapid preparation of the triplite-phase of LiFeSO_4F for use as a large-potential Fe cathode. *J Am Chem Soc* 134(44):18380–18387
- Kanagaraj AB, Chaturvedi P, Kim HJ, Choi DS (2021) Controllable synthesis of LiFePO_4 microrods and its superior electrochemical performance. *Mater Lett* 283:128737–128741
- Yang SF, Song YN, Zavalij PY, Whittingham MS (2002) Reactivity, stability and electrochemical behavior of lithium iron phosphates. *Electrochem Commun* 4(3):239–244
- Gibot P, Casas-Cabanas M, Laffont L, Lévassieur S, Carlach P, Hamelet S, Tarascon JM, Masquelier C (2008) Room-temperature single-phase Li insertion/extraction in nanoscale Li_xFePO_4 . *Nat Mater* 7(9):741–747
- Cuisinier M, Martin JF, Dupre N, Yamada A, Kanno R, Guyomard D (2010) Moisture driven aging mechanism of LiFePO_4 subjected to air exposure. *Electrochem Commun* 12(2):238–241
- Asl HY, Choudhury A (2014) Phosphorous acid route synthesis of iron tavorite phases, $\text{LiFePO}_4(\text{OH})_{1-x}\text{F}_x$ [$0 \leq x \leq 1$] and comparative study of their electrochemical activities. *RSC Adv* 4(71):37691–37700
- Sharma L, Nakamoto K, Okada S, Barpanda P (2019) Tavorite LiFePO_4OH hydroxyphosphate as an anode for aqueous lithium-ion batteries. *J Power Sources* 429:17–21
- Zhou G, Duan XC, Liu B, Li QH, Wang TH (2014) Architectures of tavorite $\text{LiFe}(\text{PO}_4)(\text{OH})_{0.5}\text{F}_{0.5}$ hierarchical microspheres and their lithium storage properties. *Nanoscale* 6(19):11041–11045
- Marx N, Croguennec L, Carlier D, Bourgeois L, Kubiak P, Le Cras F, Delmas C (2010) Structural and electrochemical study of a new crystalline hydrated iron(III) phosphate $\text{FePO}_4 \cdot \text{H}_2\text{O}$ obtained from $\text{LiFePO}_4(\text{OH})$ by ion exchange. *Chem Mater* 22(5):1854–1861
- Luo W, Wen L, Luo H, Song R, Zhai Y, Liu C, Li F (2014) Carbon nanotube-modified LiFePO_4 for high rate lithium ion batteries. *New Carbon Mater* 29(4):287–294
- Zhou X, Wang F, Zhu Y, Liu Z (2011) Graphene modified LiFePO_4 cathode materials for high power lithium ion batteries. *J Mater Chem* 21(10):3353–3358
- Wang B, Al Abdulla W, Wang D, Zhao X (2015) A three-dimensional porous LiFePO_4 cathode material modified with a nitrogen-doped graphene aerogel for high-power lithium ion batteries. *Energy Environ Sci* 8(3):869–875
- Feng S, Shen W, Guo S (2017) Effects of polypyrrole and chemically reduced graphene oxide on electrochemical properties of lithium iron (II) phosphate. *J Solid State Electrochem* 21(10):3021–3028
- Li Y, Xu G, Fan S, Ma J, Shi X, Long Z, Deng W, Fan W, Yang S (2020) Synthesis of carbon-coated $\text{LiMn}_{0.8}\text{Fe}_{0.2}\text{PO}_4$ materials via an aqueous rheological phase-assisted solid-state method. *J Solid State Electrochem* 24(4):821–828
- Chang CC, Su HK, Her LJ, Lin JH (2012) Effects of chemical dispersant and wet mechanical milling methods on conductive carbon dispersion and rate capabilities of LiFePO_4 batteries. *J Chin Chem Soc* 59(10):1233–1237
- Li XT, Yu LN, Shao HM, Zhang W (2020) Effects of mixing processes on the property of the LiFePO_4/C cathode material via high-temperature ball milling route. *Int J Mod Phys B* 34(7):2050047–2050058
- Yuan G, Bai J, Doan TNL, Chen P (2015) Synthesis and electrochemical properties of $\text{LiFePO}_4/\text{graphene}$ composite as a novel cathode material for rechargeable hybrid aqueous battery. *Mater Lett* 158:248–251
- Li YC, Zhang YP, Ma JJ, Yang L, Li XB, Zhao EQ, Fan SM, Xu GR, Yang ST, Yang CC (2019) Synthesis of LiFePO_4 nanocomposite with surface conductive phase by Zr doping with Li excess for fast discharging. *J Electrochem Soc* 166(2):A410–A415
- Zhan TT, Jiang WF, Li C, Luo XD, Lin G, Li YW, Xiao SH (2017) High performed composites of $\text{LiFePO}_4/3\text{DG}/\text{C}$ based on FePO_4 by hydrothermal method. *Electrochim Acta* 246:322–328

Publisher's Note Springer Nature remains neutral with regard to jurisdictional claims in published maps and institutional affiliations.